

# **Modeling and Multi-Objective Optimization of Continuous Protein Recovery in Liquid-Solid Circulating Fluidized Bed Ion Exchange System**

Jahirul I. Mazumder, Jesse Zhu and Ajay K. Ray

Department of Chemical & Biochemical Engineering, The University of Western Ontario, 1151 Richmond St., London, ON N6A 5B9, Canada

## **Introduction**

Advancement in biotechnology, petrochemical and metallurgical industries leads to the requirement for new types of liquid-solids reactor system which is capable of simultaneous reaction and regeneration in a continuous mode. This is particularly true for cases where the production rate is limited by the activity of the catalysts/capacity of the ion exchange particles. If catalyst/ion exchange particles can be continuously regenerated, higher productivity/throughput is achievable even using catalysts/ion exchanger with relatively low kinetics. Liquid-solid circulating fluidized bed (LSCFB) is an integrated two column system which can accommodate two separate processes (simultaneous reaction and regeneration) in the same system unit with continuous circulation of the solid particles between the two columns. LSCFB reactors provide high liquid-solid contact efficiency, favorable mass and heat transfer and reduced back mixing of phases, and are capable of treating streams containing suspended particulates (Zhu et al. 2000, Lan et al., 2000). Having these advantages, LSCFB emerges as promising liquid-solid contacting equipment in chemical and biochemical processes for both the production and the removal of contaminants from products. Lan et al. (2000; 2002) developed a LSCFB ion-exchange system for the continuous recovery of proteins from biological broths.

Comprehensive modeling and multi-objective optimization of the LSCFB system for continuous protein recovery are carried out in this study. Detailed modeling of the hydrodynamics, mass transfer and kinetics of adsorption and desorption of protein in the LSCFB ion-exchange system is fundamental and crucial for better understanding of the adsorption and desorption behaviors, the design and scale up of the LSCFB system, and optimization of the operating parameters. The only model for continuous protein recovery in LSCFB ion-exchange system was developed by Lan et al. (2000) assuming the process is limited by surface adsorption/desorption; but ion-exchange processes are generally controlled by slow diffusion. Again, detailed hydrodynamics of the LSCFB was not included in their model.

Two separate operations are carried out simultaneously in the two columns of LSCFB system and the performance of these operations are mutually dependent. Therefore, optimum design and operation of the LSCFB system for the better overall performance is very critical. Moreover, the design and operation of LSCFB system for continuous protein recovery are associated with several important objectives such as production rate, recovery, and ion exchange resin requirements, which need to be optimized. Optimization

of all individual objectives simultaneously is the best way to approach such multi-objective problems. The results of multi-objective optimization are conceptually different from single objective optimization problems. Solution of multi-objective optimization problems give an entire set of equally good solutions known as Pareto-optimal set. The choice of one solution for better performance requires additional information on the system which is often non-quantifiable. Srinivas and Deb (1995) developed non-dominated sorting genetic algorithm (NSGA) to solve multi-objective optimization problems. Later on Deb et al. (2002) incorporated elitism, a method in preserving good solution, in NSGA, which is referred as elitist non-dominated sorting genetic algorithm (NSGA-II). NSGA-II provides better convergence and better spread of Pareto-optimal solutions. Subsequently, the performance of NSGA-II has been further improved by incorporating the concept of jumping gene (JG) (portion of a chromosome string replaced by new, same-sized, randomly generated binary string) and several JG adaptations are made available (Kasat and Gupta, 2003; Agarwal and Gupta, 2008). In this study, a binary-coded NSGA-II-aJG was used for the multi-objective optimization of LSCFB ion-exchange system for continuous protein recovery.

### Modeling of LSCFB Ion Exchange System

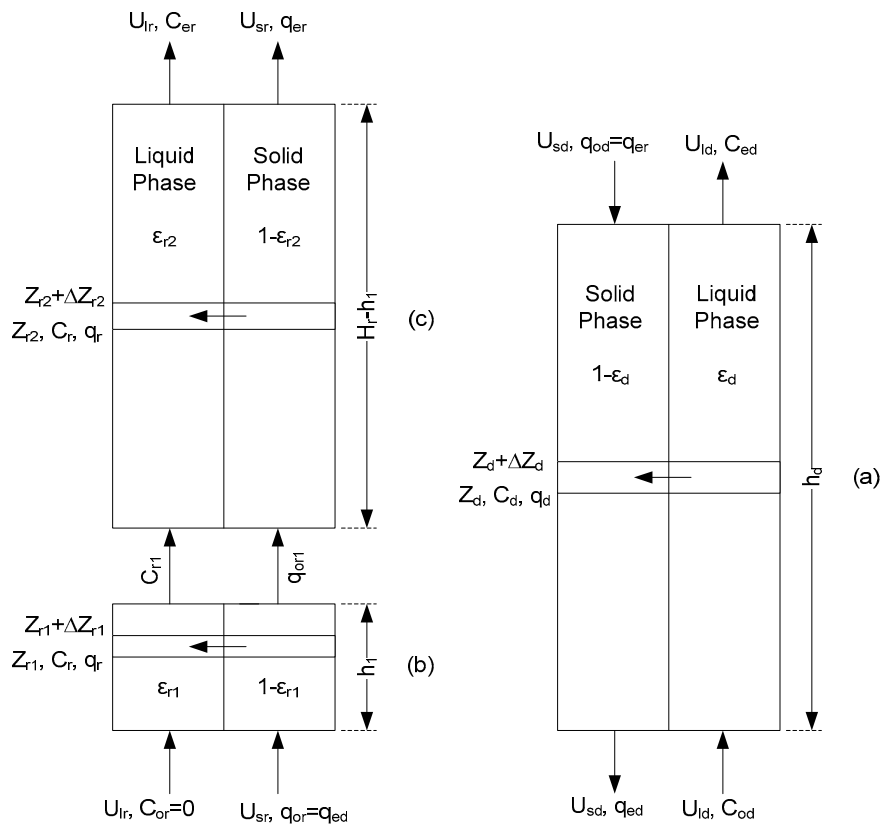


**Figure 2:** Flow patterns in (a) the downcomer, and (b) distributor zone and (c) upper dilute zone of the riser.

### Design equation for the downcomer:

Lan et al. (2002) observed three different operating zones in the downcomer which differ in solids holdup: the dense phase zone, the dilute phase zone and the freeboard zone. The protein concentration is very low in the dilute phase and the freeboard zone. Solids hold up in the dense phase zone is much higher than that of the other zones and contains most of the ion-exchange particles. Hence, the dense phase zone is considered as effective bed for adsorption.

$$U_{ld} \frac{\partial C_d}{\partial Z_d} + \psi k_f a (C_d - C_s) (1 - \varepsilon_d) = 0 \quad (1)$$

where,  $C_d$  is the protein concentration in the bulk liquid phase of the downcomer;  $U_{ld}$  is the superficial liquid velocity in the downcomer;  $Z_d$  is the axial distance from the bottom of the downcomer;  $\varepsilon_d$  is the voidage in the downcomer dense phase;  $\psi$  is a constant factor which includes the effects of intra-particle diffusion and liquid phase axial dispersion;  $a$  is the specific surface area of the ion-exchange resins.  $C_s$  is the equilibrium liquid phase protein concentration at liquid-solid interface predicted using the Langmuir isotherm:

$$C_s = \frac{K_d q_d}{q_m - q_d} \quad (2)$$

where,  $q_m$  is the maximum adsorption capacity of the ion-exchange particles,  $K_d$  is the dissociation constant,  $q_d$  is the solids phase protein concentration in the downcomer.

$$q_d = \frac{U_{ld}}{U_{sd}} (C_d - C_{ed}) + q_{od} \quad (3)$$

$k_f$  is the film mass transfer co-efficient ( $k_f$ ) in the downcomer dense phase calculated as a function of solids holdup ( $\varepsilon_{sd}$ ) and particles Reynolds number ( $Re_p$ ) using the correlation reported by Fan et al. (1960):

$$k_f = \frac{D_m}{d_p} (2 + 1.03 (\varepsilon_{sd} Re_p)^{1/2} (Sc)^{1/3}) \quad (4)$$

$$\text{where, } Re_p = \frac{d_p U_{slip} \rho}{\mu}; Sc = \frac{\mu}{\rho D_m}; u_{slip} = \frac{U_{ld}}{\varepsilon_d} + \frac{U_{sd}}{1 - \varepsilon_d} \quad (5)$$

The value of  $D_m$  for BSA solution was estimated using the following correlation reported by Young et al. (1980):

$$D_m = 8.34 \times 10^{-8} \left( \frac{T}{\mu M^{1/3}} \right) \quad (6)$$

$\varepsilon_d$  is the voidage in the downcomer dense phase and is calculated using the modified Richardson-Zaki equation:

$$U_{ld} + U_{sd} \frac{\varepsilon_d}{1 - \varepsilon_d} = U_i \varepsilon_d^n \quad (7)$$

The bed expansion index ( $n$ ) can be determined from the following correlation:

$$n = (4.4 + 18 \frac{d_p}{D_c}) \text{Re}_t^{-0.01} \quad (8)$$

$$\text{where, } \text{Re}_t = \frac{U_t d_p \rho}{\mu} \quad (9)$$

$U_i$ , the superficial liquid velocity at  $\varepsilon = 1$ , which can be determined using following empirical equation (Khan and Richardson, 1989):

$$\frac{U_i}{U_t} = 1 - 1.15 \left( \frac{d_p}{D_c} \right)^{0.6} \quad (10)$$

### Design equation for the riser:

The riser distributor separates the liquid flow into two portions: primary liquid flow and auxiliary liquid flow. Because of the arrangement of the riser distributor, two distinct zones, namely a distributor zone and an upper dilute zone, are observed along the riser based on their solids holdup.

$$\text{Distributor zone of the riser, } U_{sr} \frac{\partial q_r}{\partial Z_{r1}} + k_{r1} q_r \varepsilon_{sr1} = 0 \quad (11)$$

*Boundary Conditions:*

$$\text{At } Z_{r1} = 0 \quad C_r = 0 ; q_r = q_{or} \quad (12a)$$

$$\text{At } Z_{r1} = h_1 \quad C_r = C_{r1} ; q_r = q_{or1} \quad (12b)$$

$$\text{Upper dilute zone of the riser, } U_{sr} \frac{\partial q_r}{\partial Z_{r2}} + k_{r2} q_r \varepsilon_{sr2} = 0 \quad (13)$$

*Boundary Conditions:*

$$\text{At } Z_{r2} = h_1 \quad C_r = C_{r1} ; q_r = q_{or1} \quad (14a)$$

$$\text{At } Z_{r2} = 3 \quad C_r = C_{er} ; q_r = q_{er} = q_{od} \quad (14b)$$

where,  $k_{r1}$  and  $k_{r2}$  are desorption rate constants in the distributor zone and the upper dilute zone respectively.  $\square_{sr1}$  and  $\square_{sr2}$  are the solid hold up in the distributor zone and in the upper dilute zone of the riser, and can be calculated using the following equations:

$$U_{lr} - U_{sr} \frac{\varepsilon_{r1}}{1 - \varepsilon_{r1}} = U_i \varepsilon_{r1}^n \quad (15)$$

$$\varepsilon_{sr2} = 2.64 \times 10^{-14} U_{lr}^{-5.343} + 2.57 \times 10^{-5} G_s U_{lr}^{-1.578} \quad (16)$$

$n$  and  $U_i$  can be calculated using Eqs. (8)-(10).

## Formulation of Multi-objective Optimization

Protein adsorption and desorption are carried out in two separate columns of a LSCFB ion-exchange system with continuous solids circulation between the two columns. As the operation of one column also influence the performance of the other column, optimization of the entire system concurrently is of crucial importance to maximize the overall performance. From the view point of recovery of protein from broths, the most pertinent objectives are to maximize the fraction of protein recovered ( $R$ ) and the production rate ( $P$ ) (throughput or capacity). In terms of the operating costs another important objective is to minimize the amount of solids (resins) required ( $S$ ).  $P$ ,  $R$  and  $S$  are defined as follows:

$$P = (\text{flow rate of the extract stream}) \times (\text{protein concentration in the extract}) \\ = U_{lr} A_r C_{er} \quad (17)$$

$$R = \frac{\text{amount of protein in the extract}}{\text{amount of protein in the feed}} = \frac{U_{lr} A_r C_{er}}{U_{ld} A_d C_{od}} \quad (18)$$

$$S = \sum (\text{Amount solids in different sections of the LSCFB}) \\ = (h_d A_d \varepsilon_d + h_1 A_r \varepsilon_{r1} + (H_r - h_1) A_r \varepsilon_{r1} + V p \varepsilon_p) \rho_p \quad (19)$$

Because of the conflicting influence of decision variables on these performance parameters as seen in the sensitivity analysis, it is not possible to maximize the recovery and the production rate, and/or to minimize the amount of solids required simultaneously. One must perform a systematic multi-objective optimization study to determine the optimal operating conditions of the LSCFB ion-exchanger.

Two and three objectives optimization studies were performed to find out the optimal conditions for the operation of existing setup. Objective functions used in this study are:

$$\text{Maximize } J_1 = R \quad (20)$$

$$\text{Maximize } J_2 = P \quad (21)$$

$$\text{Minimize } J_3 = S \quad (22)$$

For optimizing the operation of the existing LSCFB unit, five adjustable (manipulative) parameters, which significantly affect the performance of the system, were chosen as the decision variables. Following are the decision variables and their bounds used for the operating stage optimization:

$$0.4 \leq U_{ld} \leq 1.2 \text{ mm/s} \quad (23)$$

$$0.6 \leq G_s \leq 1.5 \text{ kg/m}^2\text{s} \quad (24)$$

$$9.0 \leq U_{lr} \leq 21 \text{ mm/s} \quad (25)$$

$$0.5 \leq C_{od} \leq 2.0 \text{ kg/m}^3 \quad (26)$$

$$0.4 \leq h_d \leq 1.0 \text{ m} \quad (27)$$

Upper and lower bound of these operating parameters were chosen based on the stability of the system as observed by Lan et al. (2002) and mathematical feasibility.

Optimization programs used in this work are for the maximization of objective functions and hence minimization of a function ( $J$ ) was converted to maximization function ( $I$ ) by using the transformation of  $I = 1/(1+J)$ .

## Results and Discussions

### Maximization of Recovery ( $R$ ) and Production rate ( $P$ )

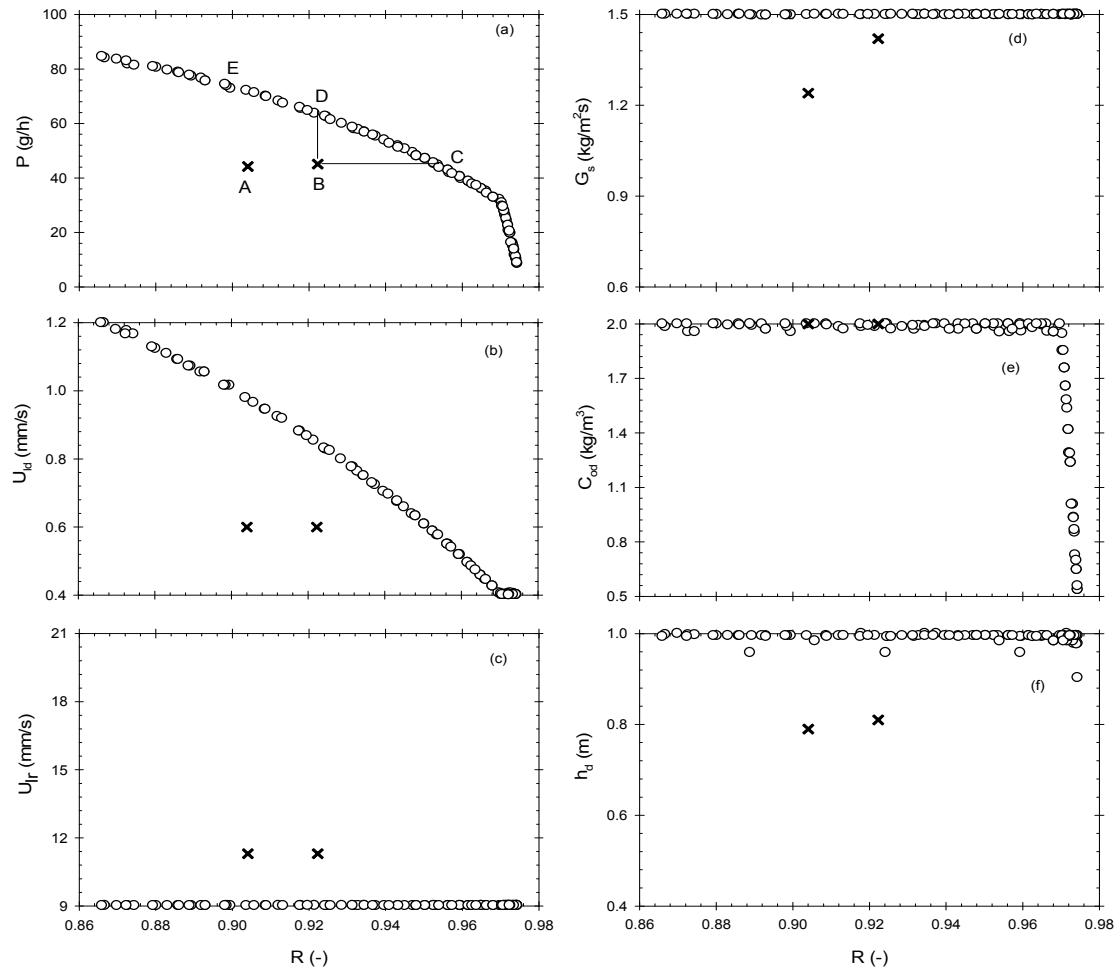


**Figure 1:** Results for two-objective optimization: maximization of production rate and recovery) (a) Pareto-optimal set; (b-f) values of decision variables corresponding to the points of Pareto-optimal set shown in part (a); x indicates current experimental operating points.

Figure 1a shows the Pareto-optimal set obtained for the simultaneous maximization of the protein recovery ( $R$ ) and the production rate ( $P$ ). It shows a contradictory behavior between the two objectives, i.e., moving from the left to the right (for example, from point E to C) the protein recovery is increased at the cost of reduced production rate. The

maximum possible recovery is very close to 1.0 while the maximum possible production rate equal to about 86 g/hr. Each point on the Pareto-optimal front corresponds to a set of decision variables, which are plotted in *Figure 1b-f* against the  $R$ . The maximum and minimum values of y-axis in the *Figure 1b-f* corresponds to the upper and lower bounds of the respective decision variables. Among the decision variables superficial liquid velocity in the downcomer ( $U_{ld}$ ) is the most sensitive one with respect to  $R$  and  $P$ , and the Pareto was mainly formed because of the conflicting behaviour of the  $U_{ld}$  on the two objective functions. *Figure 1b* shows with the decrease in  $U_{ld}$ , the recovery is increased while production rate is decreased, which was expected from the sensitivity analysis results discussed earlier. With the decrease in  $U_{ld}$ , the residence time is increased, but the protein loading rate decreased.  $U_{ld}$  reached its lower bound when  $R$  is equal to 0.97. After that sharp decrease in  $C_{od}$  contribute to the increase in  $R$ . It also resulted in sharp decrease in  $P$ . The optimum values of rest of the decision variables ( $G_s, U_{lr}, h_d$ ) obtained are constant as expected.  $G_s$  and  $h_d$  hit the upper bound as the increase in  $G_s$  or  $h_d$ , resulted in higher values of both recovery and production. On the other hand  $U_{lr}$  hit the lower bound.

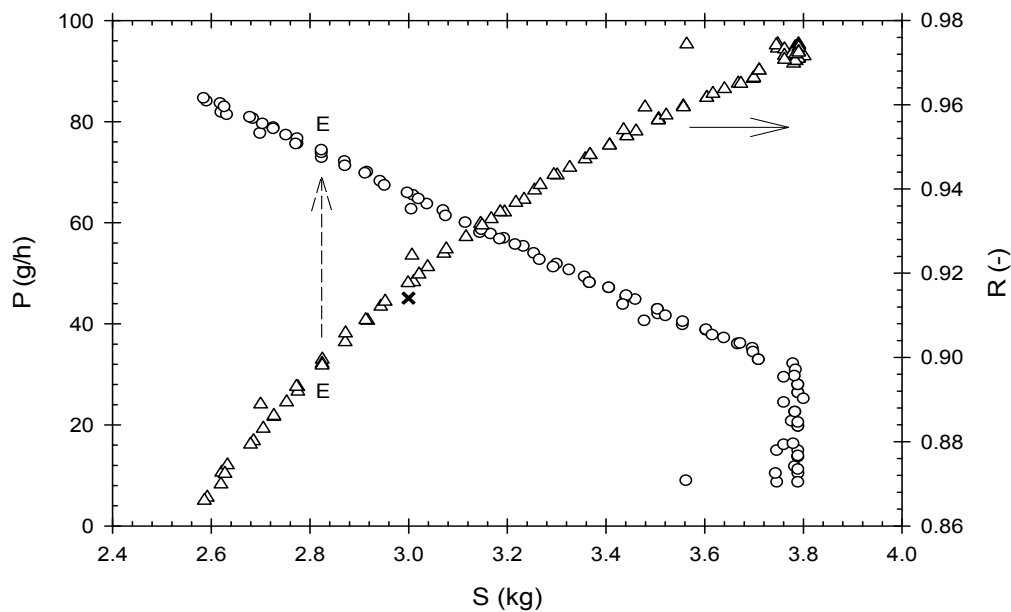


**Figure 2:** Protein production rate ( $\circ$ ) and recovery ( $\Delta$ ) against amount of the solids required ( $S$ ) for Case A (maximization of production rate and recovery). Production rate versus solids required of the current operation point B (*Figure 1*) is shown by  $x$ . E indicates points corresponding to the same point on the Pareto in *Figure 1*.

*Figure 1* also shows the current experimental operating points. Point B is better than point A in terms of both the recovery and the production rate. However, all the points on the Pareto set are much better than the current operating points. It shows that the production rate can be increased by  $\sim 43\%$  for a fixed recovery same (point D over point B) or the recovery can be improved by  $\sim 4\%$  without decreasing the current production rate (point C over D). Selection of a point from the entire Pareto sets for the efficient operation depends on other factors such as cost of the feed, downstream processing,

operating costs, etc., which are site and time specific. Of the two objectives which one is most important depends on these factors. To see the amount of particles required corresponding to the points on the Pareto set, the production rate and the recovery are plotted against the calculated values of the solids required ( $S$ ) in *Figure 2*. In case of protein recovery from the biological broth 90% recovery is acceptable. *Figure 1* and *Figure 2* show that for  $R$  equal to 0.9, the value of  $P$  increased to 74.2 g/h (point E) while the amount of solids required is less than the current experimental operating point. With a small sacrifice in the recovery, one can achieve much higher production rate using less ion-exchange resins. So, for the case of protein recovery from cheese whey, the point E is a reasonable selection. On the other hand, one also needs to remember that moving from right to left in the Pareto front will increase the pumping costs because of the increase in  $U_{ld}$ . However, *Figure 1* and *Figure 2* provide a wide range of competing options for the improvement over the current operation.

### Maximization of Production Rate ( $P$ ) and Recovery ( $R$ ), and minimization of Solids Required ( $S$ )

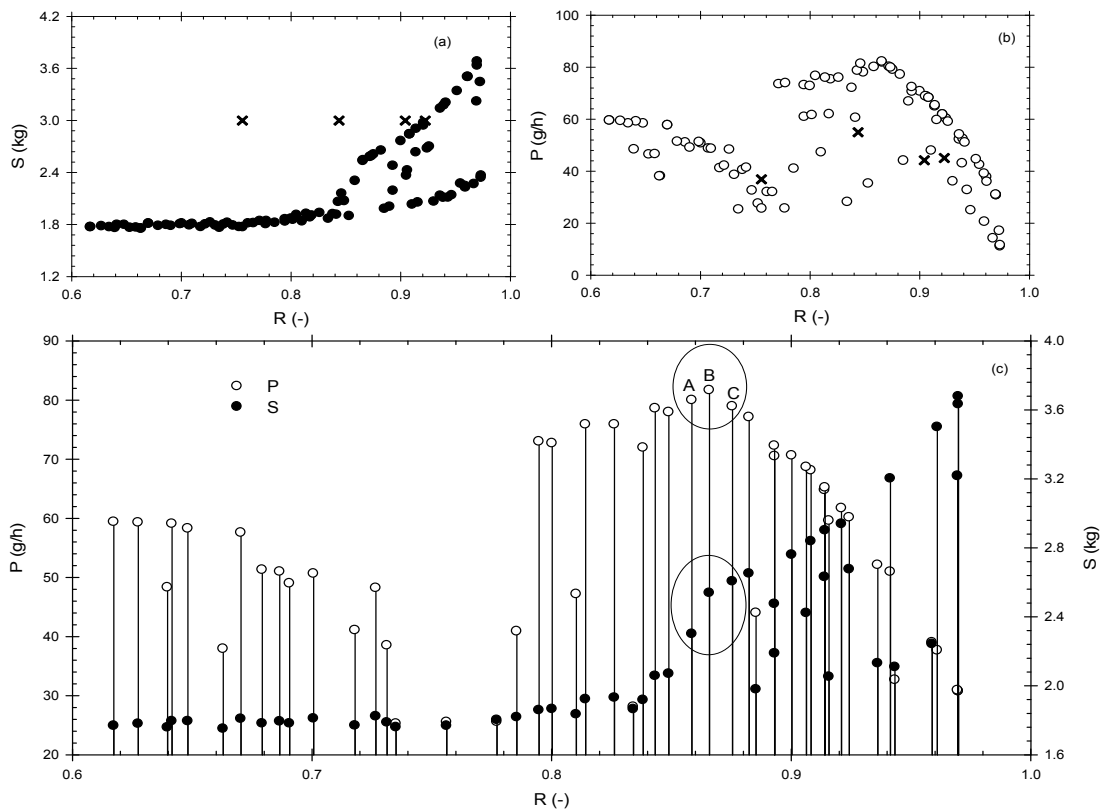


**Figure 3:** Results for three-objective optimization: (maximization of production rate and recovery, and minimization of solids required); x indicates current experimental operating points.

To obtain a clear understanding of the system performance in terms of production rate ( $P$ ), recovery ( $R$ ) and amount of ion-exchange particles required ( $S$ ), we carried out a

three objective optimization: maximization of  $P$  and  $R$ , and minimization of  $S$ , simultaneously. *Figure 3* represents the optimal Pareto set generated in this case. Solids required (*Figure 3a*) and production rate (*Figure 3b*) are plotted against the recovery. The figures show that the Pareto is wide spread and the common trend is with increasing  $R$ ,  $S$  is increased (not desired), while  $P$  is gradually increased up to a certain point and then decreased sharply. Although the plots are visually scattered, all points are non-dominating i.e., when we move one point to another in the plot at least one objective function improves and at least another deteriorates. To establish the fidelity of the non-dominance,  $S$  and  $P$  are plotted against increasing  $R$  in the same figure (*Figure 3c*). To make it clearly visible, only alternative chromosomes are plotted. It should be noted that in case of three-objective optimization, a Pareto (non-dominating) consists of points where either two objective functions improve with one deteriorating or only one objective function improving with two deteriorating. For example, in *Figure 3c*, from point A to B, both the  $P$  and  $R$  increased, but  $S$  is also increased (two improving, one deteriorating) whereas from point B to C, both  $P$  and  $S$  deteriorated, while  $R$  improved (one improving, two deteriorating). Similarly, if we compare any two chromosomes in *Figure 3c*, one would not find any pair where all three objectives improved or deteriorated. Therefore all points in *Figure 3c* are equally good (non-dominated). Once again, compare to the current experimental points, the optimal Pareto provides lot of options for improvement.

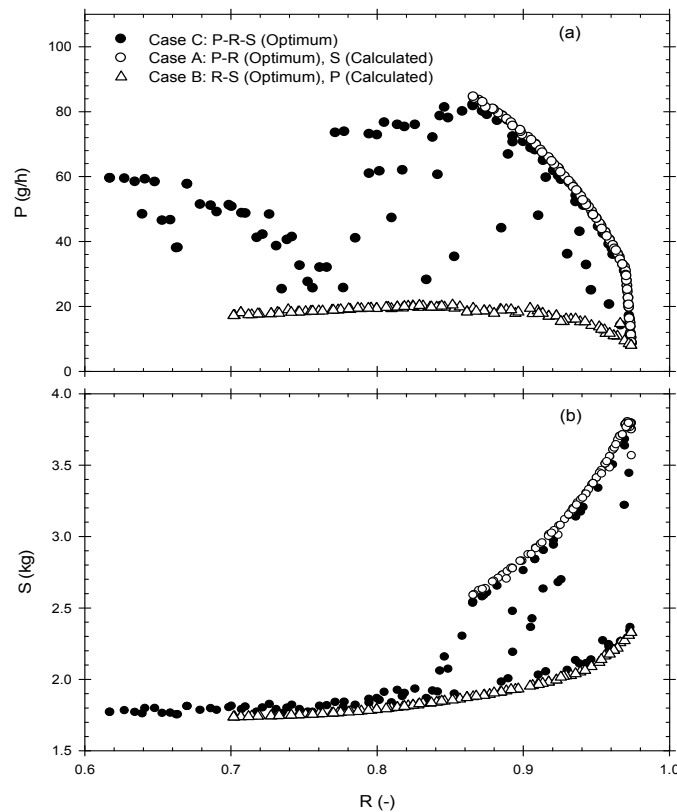


**Figure 4:** Comparison of optimization results plotted as (a) production rate vs recovery and (b) solids required vs recovery, obtained from three-objective optimization Case C (●) and two-objective optimization Case A (○) and Case B (△). (Case A: maximization of  $P$  and  $R$ ; Case B: maximization of  $R$  and minimization of  $S$ ; Case C: maximization of  $P$  and  $R$ , and minimization of  $S$ )

Three-objective optimization results are compared with the results obtained from two-objective optimizations. For both the three and two-objective optimizations, production rate ( $P$ ) and solids required ( $S$ ) are plotted against the recovery ( $R$ ) in *Figure 4*. Note that, for the Case A (maximization of  $P$  and  $R$ ) the values of  $S$  and for the Case B (maximization of  $R$  and minimization of  $S$ ) the values of  $P$  corresponding to their Pareto front are calculated and shown in the figure. *Figure 4* shows that the  $P$ - $R$  trade-off is slightly better for the two-objective optimization (Case A) than the three-objective optimization (Case C). However, the calculated values of the  $S$  corresponding to the Pareto front of the Case A are much higher than that in Case C where  $S$  was simultaneously minimized. On the other hand, Case B provides options to recover a particular fraction of proteins using less solids. Whereas in Case C one may achieve much higher production rate than that in Case B. Therefore, three-objective optimization provides better solution to achieve high recovery with improved production rate using less solids. Furthermore, three-objective optimization provides wider range of options to select the best possible solutions.

## Conclusions

A comprehensive mathematical model of the Liquid-Solid Circulating Fluidized Bed (LSCFB) ion exchange system for continuous protein recovery was developed considering the hydrodynamics of LSCFB and the ion exchange kinetics, in order to understand clearly the adsorption and desorption behaviour of the system. Subsequently, this model was used for multi-objective optimization of the system at both the operation and the design stages.

Three important performance parameters of the system were used as objective functions for multi-objective optimization study: maximization of the protein production rate, maximization of the fraction of protein recovered, and minimization of the amount of ion exchange resins required. Five operating parameters which have significant influence on the objective functions were considered as decision variables. Two- as well as three-objective function optimization were carried out to find out the optimal values of decision variables. The optimization results for all problems showed significant improvements in the system performance over the current experimental operating points. Optimization results obtained for simultaneous maximization of the production rate and the recovery of the existing LSCFB units showed that the production rate can be increased about 43% over the current experimental results using only 1% excess ion exchange resins for the same recovery level (92.2%) while for the fixed production rate (of 45 g/hr) the recovery increased by 4% over the experimental results. Whereas when all the three objectives were optimized simultaneously, for fixed recovery (of 92.2%), the production rate increased circa 33% over the current experimental results using only 89% of the existing ion exchange resins used. In design stage optimization, design parameters are also considered as decision variable in addition to operating parameters. Hence, the design stage optimization provides far more flexibility compared to the optimization of the performance of the existing unit.

## References

- Agrawal, A., Gupta, S.K., "Jumping Gene Adaptations of NSGA-II and their Use in the Multi-objective Optimal Design of Shell and Tube Heat Exchangers" *Chem. Eng. Res. & Design* 86, 123-139 (2008)
- Chang, Y.K., Chase, H.A., "Development of Operating Conditions for Protein Purification Using Expanded Bed Techniques: The Effect of the Degree of Bed Expansion on Adsorption performance" *Biotechnol. Bioeng.* 49, 512-526 (1996)
- Deb, K., Pratap, A., Agarwal, A., Meyarivan, T., "A Fast and Elitist Multiobjective Genetic Algorithm: NSGA-II" *IEEE Transactions on Evolutionary Computation* 6, 182-197 (2002)
- Fan, L-T., Yang, Y-C., Wen, C-Y., "Mass Transfer in Semifluidized Beds for Solid-Liquid System" *AICHE J.* 6(3), 482-487 (1960)
- Kasat, R.B., Gupta, S.K., "Multi-Objective Optimization of An Industrial Fluidized Bed Catalytic Cracking Unit (FCCU) Using Genetic Algorithm with the Jumping Genes Operator" *Comp. Chem. Eng.* 27, 1785-1800 (2003)
- Lan, Q.D., Zhu, J.X., Bassi, A.S., Margaritis, A., Zheng, Y., Rowe, G.E., "Continuous Protein Recovery Using a Liquid-Solid Circulating Fluidized Bed Ion Exchange System: Modeling and Experimental Studies" *Can. J. Chem. Eng.* 78, 858-866 (2000)
- Lan, Q.D., Zhu, J.X., Bassi, A.S., Margaritis, A., "Continuous Protein Recovery with a Liquid-Solid Circulating Fluidized Bed Ion Exchanger" *AICHE J.* 48, 252-261 (2002)
- Srinivas, N., Deb, K., "Multi-Objective Function Optimization Using Non-Dominated Sorting Genetic Algorithms" *J. Evolutionary Computation* 2, 221- 248 (1995)
- Zhu, J-X., Zheng, Y., Karmanev, D., Bassi A.S., "(Gas-) Liquid – Solid Circulating Fluidized Beds and their Potential Applications to Bioreactor Engineering" *Can. J. Chem. Eng.* 78, 82-94 (2000)